

PERFORMANCE EVALUATION OF A THREE-STOREY UNREINFORCED MASONRY BUILDING DURING THE 1992 ERZINCAN EARTHQUAKE

HALUK SUCUOĞLU AND ALTUĞ ERBERİK

Earthquake Engineering Research Center, Department of Civil Engineering, Middle East Technical University, 06531 Ankara, Turkey

SUMMARY

Seismic performance of a three-storey unreinforced masonry building which survived the 1992 Erzincan earthquake without damage is evaluated. Mechanical properties of the masonry walls have been determined experimentally by using identical brick and mortar used in construction. An accurate material model is developed for masonry and employed in a computer program for the non-linear dynamic analysis of masonry buildings. The analytical results based on measured material properties indicated that masonry buildings which satisfy basic seismic code requirements possess remarkable lateral strength, stiffness and energy dissipation capacity. Accordingly, a simple elastic design approach is rendered suitable for unreinforced masonry under seismic excitations, provided that realistic material properties are employed in design.

KEY WORDS: unreinforced masonry; Erzincan earthquake; damage model; wall ratio; non-linear analysis

INTRODUCTION

Structural masonry is a challenge to earthquake engineers for several reasons. The most important reason is perhaps the difficulty in the standardization of structural forms, materials and workmanship employed in masonry construction. They all depend strongly on local traditions. Moreover, mechanical properties of masonry are more complicated than its modern counterparts, steel and concrete, especially under dynamic effects.

An important portion of the building stock in the world, including seismic zones, is constituted of unreinforced masonry buildings. They will undoubtedly retain their share in the future especially in the developing countries because of the inherent advantages in material availability, construction simplicity and economic feasibility. Seismic design codes usually adopt simple yet conservative measures for unreinforced masonry construction in seismic zones as a natural consequence of high variability in their structural properties and poor earthquake performance in the past. A considerable amount of analytical and experimental research has been carried out in the last two decades for improving the seismic safety of structural masonry. However, sufficient emphasis has not been given to the performance evaluation of existing masonry buildings which survived major earthquakes. Post earthquake surveys and investigations usually keep the attention on severely or moderately damaged masonry buildings and apparent causes of their damage.^{1–3} On the other hand, the causes of survival of masonry buildings with light or no damage during earthquakes deserve similar attention because they hold the secret of ‘what is right?’ rather than the more obvious ‘what was wrong?’. The published research in this direction is very limited.^{4,5}

An earthquake of magnitude 6.8 caused substantial damage in the city of Erzincan, Turkey on March 13, 1992. The city with a population of 92 000 is located on the eastern part of the North Anatolian Fault Zone. Erzincan was completely destroyed in 1939 by the strongest earthquake of Turkish history, with a death toll of 32 000. The only building which survived the 1939 earthquake is the train station, a two-storey block-stone



Figure 1. The investigated unreinforced masonry building

masonry building which is still in service today. In the 1992 earthquake, 8 percent of the 15 000 buildings in the city collapsed or were heavily damaged.⁶ Highest damage density was in multistorey reinforced concrete frame buildings typically having 4–6 storeys. The 8000 unreinforced masonry buildings, distributed as 6120 single storey, 1700 two-storeys and 180 three-storeys, generally performed well with the exception of a complex of 40 two-storey houses constructed with non-load bearing hollow insulation bricks. They either collapsed completely or were heavily damaged.

A three-storey masonry office building, which is the subject of this study had been inspected by the authors at the aftermath of the 1992 earthquake (Figure 1). The building was constructed in 1974 by its owner, the Directorate of Forestry, in conformity with the 1968 Turkish Seismic Design Code.⁷ The observed damage in the building was thin inclined plaster cracking on two first storey walls (elements 10 and 11 in Figure 2) and flexural cracking of a reinforced concrete lintel beam connecting wall elements 1 and 15.

The earthquake ground motion was recorded at a seismograph station which is 3 km away from the epicenter and only 500 m away from the investigated building. Since soil properties are uniform throughout the city, it is reasonable to assume that the building is excited by the recorded ground motion at its base. The acceleration time histories and acceleration response spectra of the East–West and North–South components of Erzincan ground motion are shown in Figure 3.

In the presented study, non-linear dynamic response of the three-storey masonry building is calculated under the Erzincan ground excitation, and calculated performance is correlated with the observed state of the building after the earthquake. The lateral resistance capacity of the building is further evaluated by employing incremental collapse analysis and dynamic analysis procedures. Accordingly, its overstrength with respect to the design resistance and response reduction due to inelastic behaviour are estimated. This study aims at understanding the seismic behaviour of an existing masonry building by analytical simulation of its earthquake performance under an experienced earthquake excitation.

PROPERTIES OF THE INVESTIGATED BUILDING

The unreinforced masonry building shown in Figure 1 has almost identical plan dimensions and wall thicknesses in all three storeys as sketched in Figure 2. Each storey has a height of 3 m. The total areas of wall elements oriented in the NS and EW directions are 12.3 and 11.6 m², respectively. These areas correspond to wall ratios of 6.5 and 6.1 percent with respect to the total plan area of 190.5 m².

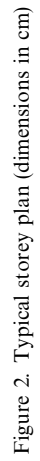


Figure 2. Typical storey plan (dimensions in cm)

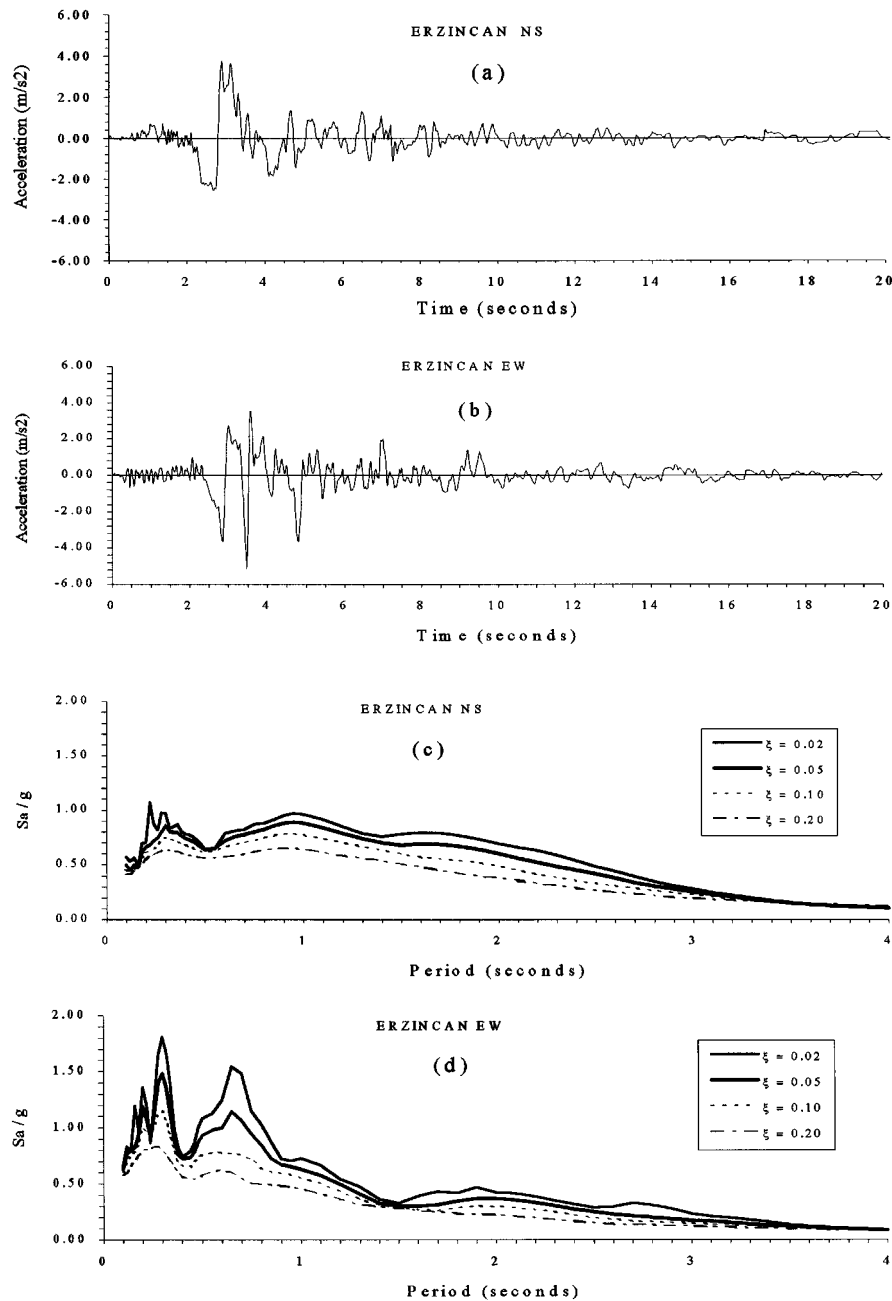


Figure 3. Erzincan earthquake horizontal ground motion components: (a) NS ground acceleration; (b) EW ground acceleration; (c) elastic acceleration response spectra, NS; (d) elastic acceleration response spectra, EW

The total masses in the first, second and third storeys are calculated as 212, 198 and 135 t, respectively. They include half of the wall masses from the storeys below and above, the mass of the 12 cm thick floor diaphragms, mass of the quarter of design live load intensity (3.5 kN m^{-2}) on the first two floors, and roof mass on the third floor. The centre of mass calculated for each storey has the co-ordinates (12.53, 5.78 m) as marked in Figure 2 whereas the mass moment of inertia of the floors are calculated as 13 816, 12 755 and 8212 kg m^2 , respectively.

Table I. Compressive test specimens and test results

Properties of the specimens	Brick unit	Mortar cube	Slender prism	Squat prism
Number of specimens	10	5	5	5
Specimen dimensions (cm)	9 × 19 × 6	5 × 5 × 5	9 × 19 × 52	19 × 19 × 26
Mean strength (MPa)	9.9	6.4	3.93	3.98
Standard deviation (MPa)	1.74	0.57	0.21	0.68
Mod. of elasticity (MPa)			998	1474

Masonry buildings in Turkey are constructed by using clay brick units produced either at local furnaces, or at brick factories. Local bricks are burned at lower temperatures (maximum 900 °C), consequently their compressive strengths are lower than the factory bricks. On the other hand, their fracture is less brittle and they can undergo considerable plastic strains prior to failure. The investigated building was constructed by clay brick units with the dimensions of 6 cm × 9 cm × 19 cm, produced at a local furnace. The mortar casted by masons used to lay these bricks has a mixture ratio specified in practice as five volumes of sand, one volume of cement and one volume of hydrated lime powder. This is the Type C mortar specified in the Turkish masonry code⁸ which approximately corresponds to the Type N mortar in the UBC⁹ with a minimum compressive strength of 5 MPa.

In order to determine the *in situ* material properties of the masonry building, similar bricks from a local furnace at the site had been delivered, and mortar had been prepared in the laboratory with the same mixture ratio. Compressive strengths of brick units and mortar cubes (28 d) were determined as reported in Table I. In addition, two types of masonry prisms were prepared for determining the compressive strength and modulus of elasticity of the walls. The slender prisms were made of eight brick layers layed in stack bond with a thickness of 9 cm and the squat prisms were made of four double brick layers in running bond with a thickness of 19 cm. The results of prism compression tests are also given in Table I.

The tensile, or diagonal cracking strength of the walls had been determined by testing three square panel specimens loaded under diagonal compression as shown in Figure 4 until the panels split diagonally. A theoretical relationship is proposed between the diagonal failure load P'_d and the tensile strength f'_t , which is based on the assumptions that the panel is homogeneous, and diagonal cracking initiates in the middle of the panel due to the combination of principal compressive and tensile stresses in accordance with the Coulomb–Mohr failure criterion:¹⁰

$$f'_t = 0.5187 f'_m \frac{P'_d}{(f'_m b t - 1.683 P'_d)} \quad (1)$$

Here, f'_m is the compressive strength of masonry, b and t are the length and thickness of the square panel, respectively. The properties of the panel specimens, test results and the tensile strength values evaluated in view of Equation (1) are presented in Table II. A mean compressive strength value of 3.95 MPa obtained from slender and squat prism test results has been employed in equation (1) for f'_m .

ANALYTICAL MODELLING

General purpose computer programs for the dynamic analysis of masonry structures are very limited, perhaps due to the wide range of variability in masonry structural forms and material characteristics. One such program^{11,12} has been developed to predict the non-linear seismic response of unreinforced masonry buildings subjected to dynamic base excitations, and employed herein. The program models the floor slabs as rigid diaphragms. Accordingly, two translational and one rotational (torsion) degrees of freedom are assigned to each floor level at the master point, which is at the mass centre of the floor diaphragm. The structural system consists of individual vertical planar wall elements continuous between the floor dia-

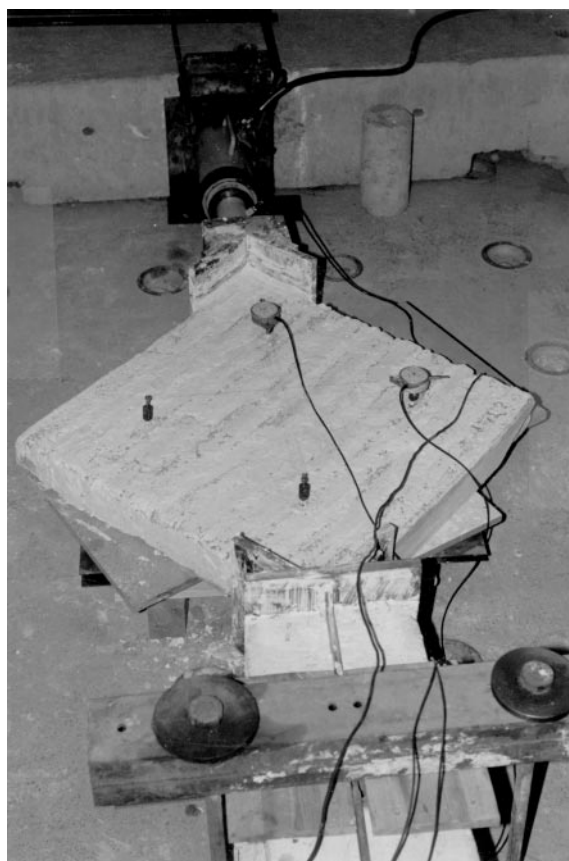


Figure 4. Diagonal loading tests of square panels

Table II. Square panel specimens and test results

Number of specimens	b (cm)	t (cm)	Mean P_d (kN)	Standard deviation (kN)	Mean f'_t (MPa)
3	85	9	66.7	5.53	0.72

phragms. In the analysis, it is assumed that non-linear behaviour arises from the shear deformation of wall elements within their own planes. This type of idealization is called the storey mechanism model which has been employed by other researchers^{13,14} for non-linear seismic analysis of masonry buildings. The type of idealization and modelling used is applicable only to masonry buildings with rigid floor diaphragms as mentioned above, but not to those buildings with flexible floors in which out of plane bending of walls is important. In particular, inadequately supported wall elements under low vertical stresses may fail in the out-of-plane bending mode in unreinforced masonry buildings, which in turn changes the global response significantly.

The investigated building has been modelled by using 27 wall elements at each storey. The L- and T-shaped wall segments shown in Figure 2 have been divided into two adjacent orthogonal wall elements with rectangular cross-sections.

Material model

In the storey mechanism model, determination of shear force–shear deformation relationships for wall elements is crucial because storey displacements directly depend on the shear deformations of wall elements. Measuring or predicting the shear behaviour of unreinforced masonry walls however is not simple especially under reversed loading. Although there are proposed hysteresis rules based on experimental observations,^{13–16} a shear stress–strain envelope curve is required for the particular wall material. Shear stress–strain curves obtained under monotonic loading until failure may be employed to represent the envelope curves when cyclic test results are not available.

The three square panel elements tested under diagonal compression to determine the tensile strength of masonry, as presented in Figure 4 and Table II, are also employed for obtaining the shear stress–strain envelope relationship of wall elements in this study. The main reason for such a replacement is the ultimate simplicity of testing a square panel under diagonal compression compared to testing a wall element under shear and vertical compression. Average shear deformation of a central macro element in each square panel specimen is measured by using two orthogonal LVDTs as shown in Figure 5. Average shear stresses acting along the boundaries of the macro element are calculated by finite element analysis in proportion to the diagonal load P_d (Figures 5(a) and 5(b)). Then average shear stress–shear strain relationship for the macro element is obtained as shown in Figure 6. This curve represents the mean relationship obtained from three square panel specimens.

It is revealed in Figure 6 that square panel reaches its ultimate shear resistance after developing a significant amount of plastic shear strain which is accompanied by diagonal splitting. The state of stress at the middle of the diagonally loaded panel is shown in Figure 5(c). Diagonal splitting initiates at this point according to Coulomb–Mohr failure criterion which is confined by biaxial compressive stresses. As shear stress increases, confining stresses also increase by maintaining a constant σ_0/τ_0 ratio of 0.53.¹⁰ This is the reason for significant plastic straining before the panel splits diagonally, which is not the case for a wall element. A wall element is subjected to constant vertical stresses and monotonically increasing shear stresses at the top and bottom boundaries as shown in Figure 7(a). Ultimate shear strength of the wall is reached when an inclined cracking initiates at the middle of the wall due to the stress state shown in Figure 7(b). Average shear stress $\bar{\tau}_{av}$ along the boundary which causes inclined cracking at the middle according to Coulomb–Mohr failure criterion can be expressed as follows:¹⁷

$$\bar{\tau}_{av}^2 = \left\{ \frac{f'_m \cdot f'_t}{[1.5(f'_m + f'_t)]^2} [f'_m f'_t + \sigma_y(f'_m - f'_t) - \sigma_y^2] \right\} \quad (2)$$

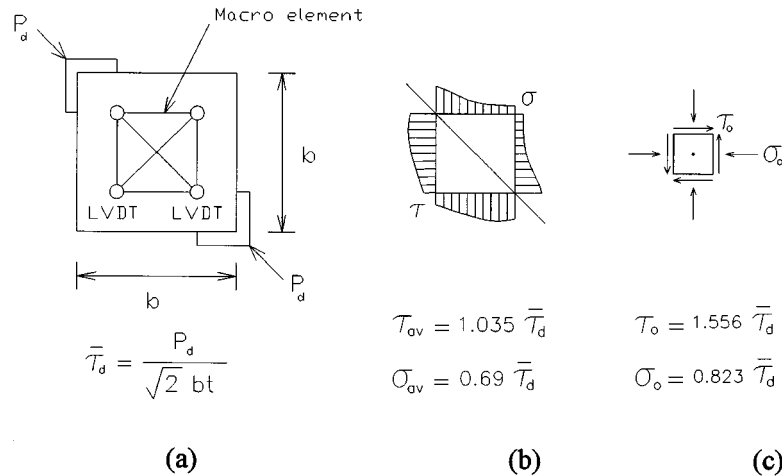


Figure 5. Stress measurements in a square panel: (a) square panel; (b) macro element; (c) stress state at the centre of square panel

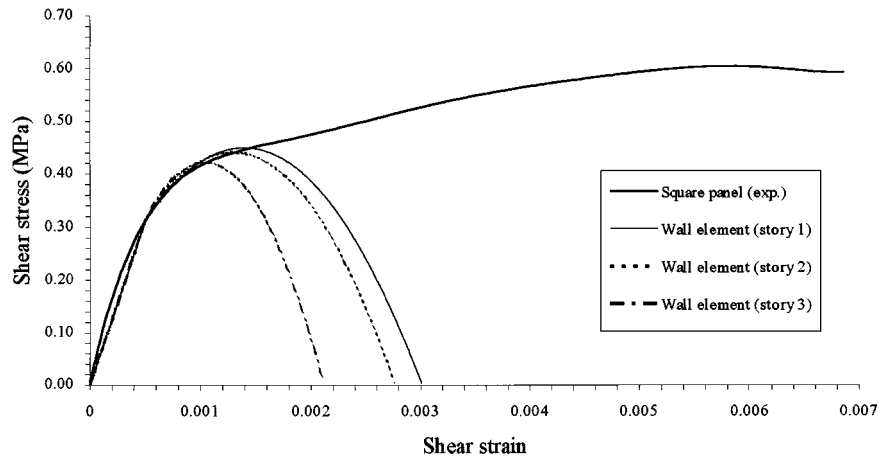


Figure 6. Mean shear stress–shear strain relationship obtained from square panel tests, and postulated relationships for the three storeys

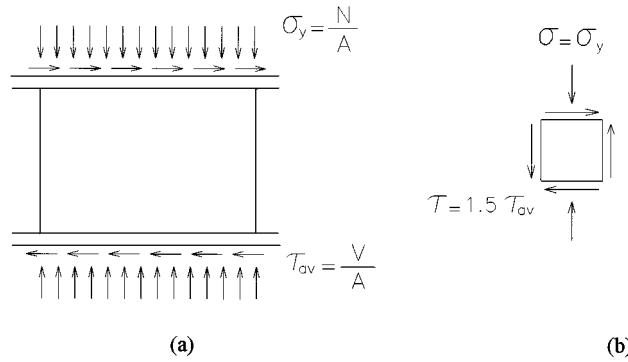


Figure 7. Stresses acting on a typical wall element: (a) average stresses along the boundaries; (b) stress state at the centre

This equation predicts failure as a result of a critical combination of principal tensile and compressive stresses σ_1 and σ_3 , i.e.

$$\frac{\sigma_1}{f'_t} - \frac{\sigma_3}{f'_m} = 0 \quad (3)$$

Another expression proposed by Turnsek and Cavocic¹⁸ predicts shear failure according to tension failure criterion, which occurs when $\sigma_1 = f'_t$. For the stress state in Figure 7(b), this criterion gives

$$\bar{\tau}_{av} = \frac{f'_t}{1.5} \sqrt{1 + \frac{\sigma_y}{f'_t}} \quad (4)$$

Although equation (4) is simpler, its prediction is less conservative than that of equation (2). Considering that the average vertical stresses σ_y in the first, second and third storeys of the investigated building are 0.218, 0.169 and 0.070 MPa, respectively, the ultimate, or cracking shear stresses calculated by equation (2) are 0.45, 0.44 and 0.42 MPa as shown in Figure 6, whereas those calculated by equation (4) are 0.55, 0.53 and 0.50 MPa for the three consecutive storeys, respectively. The ultimate shear stress values obtained by equation (2) are used here.

The initial portion of the stress-strain curve obtained for the macro element of a square panel is selected as the rising portion of the stress-strain curve of a wall element. This selection is based on the similarity of stress states acting on the two elements at various stress levels. In the low shear stress level where linear elastic behaviour prevails, the shear modulus is independent of the compressive stress level which is also confirmed by experiments.¹⁹ A shear stress value of 0.31 MPa can be selected as the limit of linear elastic behaviour from Figure 6. The stress paths for the wall elements of first, second and third storeys are presented in Figure 8 on the shear-compression plane, bounded by the diagonal cracking or ultimate shear stress level defined by equation (2). The stress path for the macro panel element is also shown in the same figure. It can be observed that the stress states of wall elements at the first two storeys are very similar to that of the macro element within the shear stress range between the elastic limit and the ultimate limit (equation (2)) of the wall elements.

The dynamic analysis program used in this study for predicting the non-linear seismic response of unreinforced masonry buildings^{11,12} employs a shear stress-strain envelope relationship as

$$\tau = \bar{G}\gamma \quad \text{for } |\gamma| \leq \bar{\gamma} \quad (5a)$$

$$\tau = \bar{G}\bar{\gamma} \left\{ 1 + (c - 1) \frac{(|\gamma| - \bar{\gamma})}{(\gamma_c - \bar{\gamma})^2} (2\gamma_c - \bar{\gamma} - |\gamma|) \right\} \frac{\gamma}{|\gamma|} \quad \text{for } |\gamma| > \bar{\gamma} \quad (5b)$$

Here, \bar{G} is the elastic shear modulus, $\bar{\gamma}$ is the elastic shear strain limit, γ_c is the shear strain at ultimate shear stress, and c is the ratio of ultimate shear stress τ_u to elastic shear stress limit τ_e . The computer software developed in References 11 and 12 uses equation (5) as the skeleton curve and supplies it with loading and unloading conditions. These conditions involve the assumption that, in view of the experimental data presented in Reference 15, the unloading behaviour of a masonry wall panel is linearly elastic.

The values of \bar{G} , $\bar{\gamma}$, γ_c , c , τ_u and τ_e which appear in equations (5) are given in Table III for the three storeys of the building and the corresponding stress-strain curves are presented in Figure 6 for the wall elements of these three storeys. Their rising portions match perfectly well with the curve obtained from experimental data. The descending portions are hypothetical since unreinforced masonry walls fail in shear almost suddenly after the formation of diagonal cracking.

Energy dissipation is modelled by viscous damping mechanism in the computer program.^{11,12} This is consistent with the non-linear behaviour of unreinforced masonry because it has negligible energy dissipation capacity due to material hysteresis under cyclic shear. Internal friction is the dominant dissipative

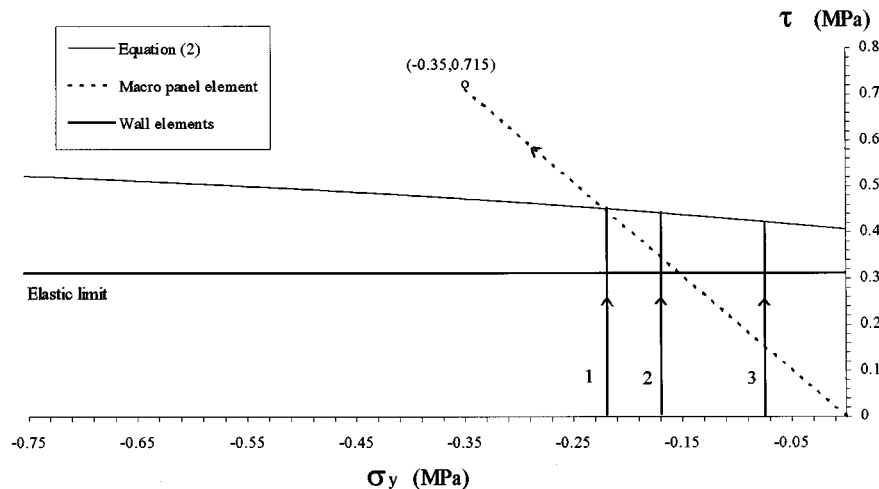


Figure 8. Shear stress-normal stress paths for wall and macro panel elements

mechanism which increases with shear strain and consequent internal micro cracking. Damping ratio varies with the secant shear stiffness and its viscous counterpart in the program, which in turn depends on shear strain history. In the model proposed in References 11 and 12, it is assumed, in view of the experimental data presented in Reference 15, that the damping coefficient (viscous coefficient associated with shear modulus) is constant in the linear range (i.e. when $|\gamma| \leq \bar{\gamma}$). On the other hand, it varies linearly with strain in between elastic and ultimate states (i.e. $\bar{\gamma} < |\gamma| < \gamma_c$). Viscous damping ratio is adjusted to 0.10 in the presented study in the linear elastic range. Its variation with the shear strain amplitude is calculated and presented in Figure 9. The damping ratio remains constant during a strain cycle.

Damage model

Unreinforced masonry walls do not possess a reliable post-cracking deformation capacity. Upon the formation of diagonal cracking when their ultimate shear capacity is reached, their strength and stiffness quickly deteriorate during subsequent cycles of loading with increasing shear strains. Therefore, a damage criterion which is based on ductility or post-cracking deformability is not appropriate for unreinforced masonry wall elements. A damage ratio is introduced here for a wall element based on the proportion of degraded stiffness to initial shear stiffness, simply defined as

$$d_i = \frac{\bar{G} - G_i}{\bar{G}} \quad (6)$$

where G_i is the secant shear stiffness of the i th element attained during a stress–strain cycle. The variation of G_i with the shear strain amplitudes of strain cycles can be derived from equations (5), by dividing both sides of the equations by the strain amplitude γ . The result obtained for the first storey wall elements is presented in Figure 10, with the simultaneous variation of wall damage ratio calculated in view of equation (6). It may be

Table III. Parameters defining shear stress–shear strain relationships of wall elements

Story	\bar{G} (MPa)	$\bar{\gamma}$	γ_c	c	τ_e (MPa)	τ_u (MPa)
1	620	0.0005	0.0014	1.45	0.31	0.45
2	620	0.0005	0.0013	1.42	0.31	0.44
3	620	0.0005	0.0011	1.36	0.31	0.42

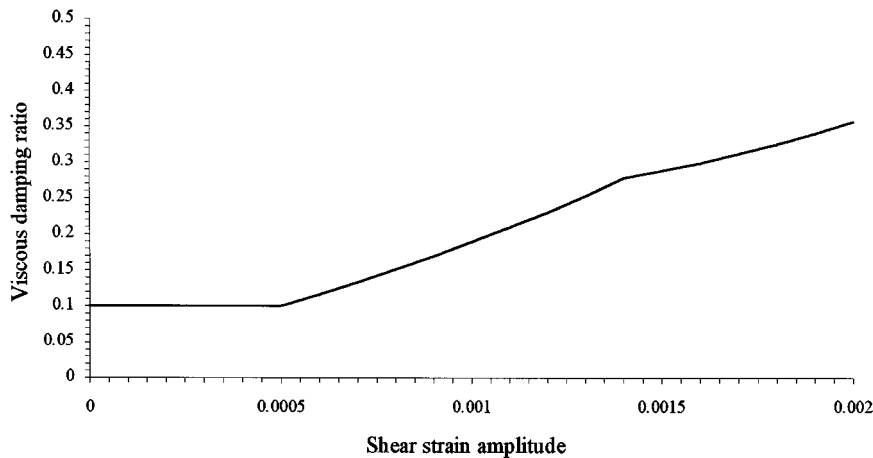


Figure 9. Variation of viscous damping ratio with the shear strain amplitude

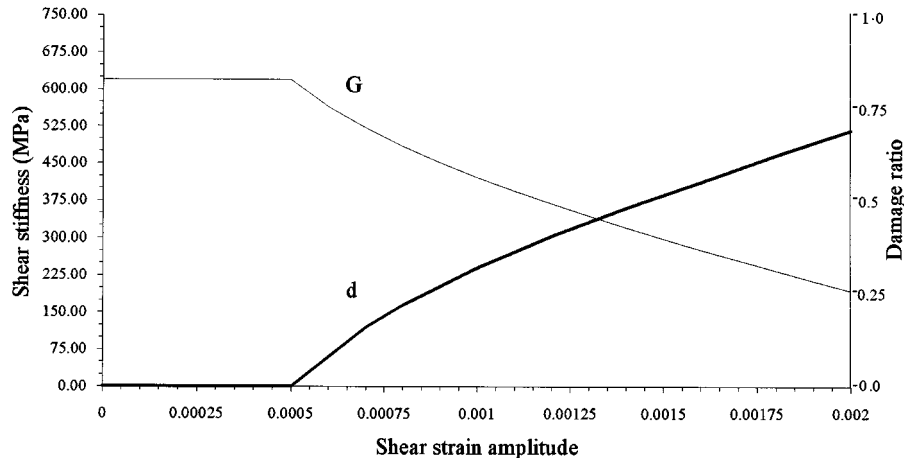


Figure 10. Variation of shear stiffness and damage ratio with the shear strain amplitude in a typical wall element

proposed that a wall element is undamaged in the linear elastic range ($d_i = 0$); lightly damaged in the inelastic range before the formation of visible cracking on the wall surface ($d_i < 0.25$); moderately damaged when inclined cracking is visible, but not completely diagonal ($0.25 < d_i < 0.50$), and heavily damaged after the formation of complete diagonal cracking ($d_i \geq 0.50$). These limits are calibrated with the results of masonry pier tests obtained under increasing cyclic shear displacements.²⁰ Although the test specimens were reinforced in Reference 20, reinforcement was effectively activated only after the formation of diagonal cracking which corresponds to heavy damage in a companion unreinforced specimen.

A damage ratio for an entire storey can be assigned in a given direction by calculating the weighted average of the damage ratios of individual wall elements at a deformation state.

$$D = \frac{\sum d_i A_i}{\sum A_i} \quad (7)$$

Here, A_i is the shear area of the i th element and summation is on those elements oriented in either the X or Y directions. The damage limits defined above are also applicable to the total damage ratio in a storey.

DYNAMIC RESPONSE ANALYSIS

Four types of analysis are carried out in this section. They are free vibration analysis, modal spectrum analysis, quasi-static incremental collapse analysis and non-linear time-history analysis.

Free vibration analysis

Modal vibration frequencies, periods and displacements of the master point at each floor are given in Table IV for the first three modes.

Effective modal masses of the first three modes account for 90 percent of the total translational and rotational masses. The frequencies of vibration in the next six modes of vibration are 21.15, 21.80, 25.06, 28.99, 29.75 and 34.00 Hz, respectively.

From the results in the table, it is observed that the frequencies of the first three modes are closely spaced. Hence, they all contribute to the total response with similar significance. Further, there is a considerable coupling between translational and rotational degrees of freedom at all three modes.

Modal spectrum analysis

Response spectrum analysis is carried out under NS and EW components of the Erzincan ground motion spectra with 10 percent damping, which act along the X and Y directions of the building, respectively. All

Table IV. Modal properties of the investigated building

Mode 1 $f = 7.94 \text{ Hz}; T = 0.13 \text{ s}$			Mode 2 $f = 8.31 \text{ Hz}; T = 0.12 \text{ s}$			Mode 3 $f = 9.52 \text{ Hz}; T = 0.11 \text{ s}$		
$U_x \text{ (m)}$	$U_y \text{ (m)}$	$R_z \text{ (rad)}$	$U_x \text{ (m)}$	$U_y \text{ (m)}$	$R_z \text{ (rad)}$	$U_x \text{ (m)}$	$U_y \text{ (m)}$	$R_z \text{ (rad)}$
0.0191	0.0114	0.0014	0.0140	− 0.0191	− 0.0007	0.0049	0.0108	− 0.0026
0.0369	0.0210	0.0025	0.0272	− 0.0362	− 0.0015	0.0099	0.0210	− 0.0051
0.0445	0.0258	0.0030	0.0335	− 0.0442	− 0.0018	0.0133	0.0247	− 0.0063

Table V. Base shear forces obtained under Erzincan spectral excitation

Excitation direction	$V_x \text{ (kN)}$	$V_y \text{ (kN)}$
NS (X)	2100	536
EW (Y)	622	3214
Combined	2286	3375

nine modes are included in the analysis and modal responses are combined with the CQC method. Further, maximum responses in each direction are combined due to the 30 percent rule. Base shear forces obtained in both orthogonal directions are presented in Table V.

The maximum shear stress in the first storey in X direction is obtained in element 3 as 0.224 MPa. The corresponding value in the Y direction is 0.341 MPa in element 11. Considering that the average stresses in the X and Y directions are 0.196 and 0.274 MPa, respectively, it may be concluded that the building distributes storey shear forces to its wall elements fairly uniformly.

Quasi-static collapse analysis

Non-linear incremental quasi-static collapse analyses are conducted in order to investigate the strength and deformability capacities of the building in the NS (X) and EW (Y) directions. A triangular lateral force distribution is imposed with increasing amplitudes at each increment. Lateral force components are applied at the master points of the stories.

Figure 11 shows the relationships between base shear force and roof displacement in both directions. The building has elastic base shear coefficients (base shear/weight) of 0.62 and 0.64, and ultimate base shear coefficients of 0.98 and 1.00 in the X and Y directions, respectively. These values are remarkable. Since the maximum design base shear coefficient of a masonry building according to the Turkish Seismic Code is 0.2, an elastic overstrength ratio of 3.1 is obtained for the investigated building. Overall drift ratio (roof displacement/building height) at the ultimate strength level is 0.00073 in both directions. These results indicate excessive rigidity of the building.

The progress of total damage in the first storey, defined by equation (7), is calculated at each load increment and presented in Figure 12 as a function of the roof displacement in order to facilitate comparison with the lateral resistance. Although the building possesses higher strength and stiffness in the Y direction, the calculated damage is less than that obtained in the X direction at similar displacements. This is due to different eccentricities in two directions. The eccentricity of the elastic resisting forces oriented in the Y direction is 1.28 m whereas eccentricity in the X direction is 0.78 m. Accordingly, damage distribution is more uniform in the X direction than the Y direction. For example, when maximum lateral strength is attained in the X direction, first storey damage index is 0.46 and damage indices of the individual wall elements vary between 0.42 and 0.48. On the other hand, first storey damage index in the Y direction at the same displacement is 0.42 whereas damage indices of wall elements vary between 0.25 and

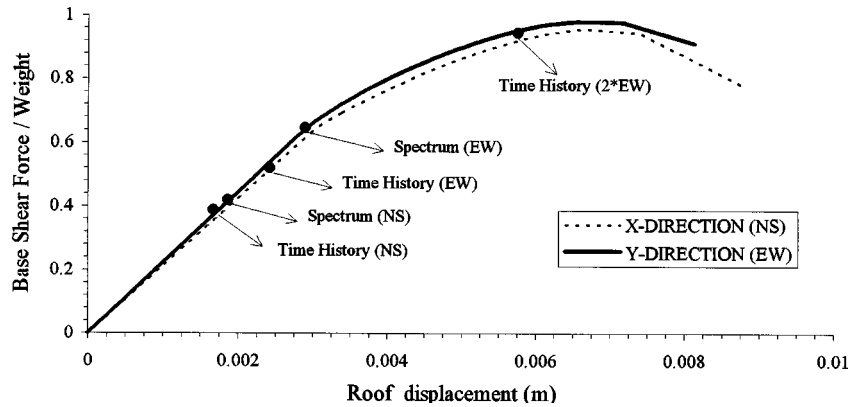


Figure 11. Base shear force variation with roof displacement under quasi-static monotonic loading

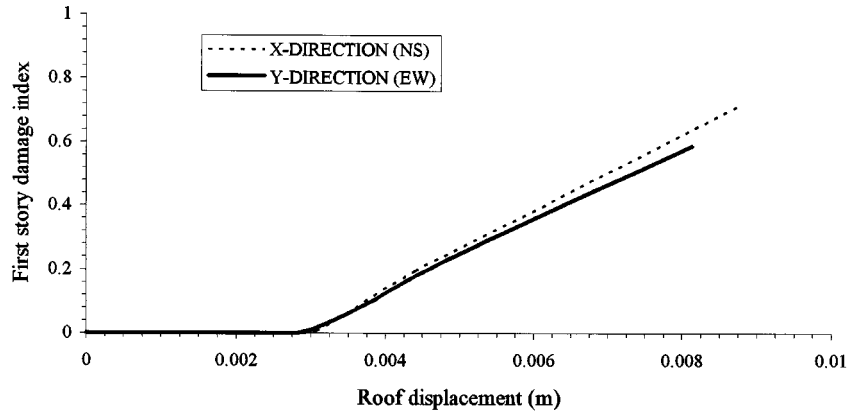


Figure 12. Variation of first-storey damage index with roof displacement under quasi-static monotonic loading

0.57. Element 8, 9, 10, 11 exhibit the highest damage value of 0.57 under monotonic loading in the positive Y direction.

The base shear force components and corresponding roof displacements obtained under Erzincan spectral excitation are also marked in Figure 11. It is observed that spectral forces do not drive the building into the inelastic range.

Time-history analysis

Dynamic response of the building is calculated under NS and EW components of the Erzincan earthquake (Figure 3). The variations of roof displacement and base shear force with time in the EW direction are shown in Figures 13(a) and 13(b), respectively, with solid lines. All elements of the building remain in the linear elastic range under both excitation components. Peak responses in two directions are indicated in Figure 11.

In order to observe the inelastic dynamic response of the building, amplitudes of the EW component of Erzincan ground acceleration are scaled by two, and time-history analysis is repeated. Roof displacement and base shear force variations obtained under the increased excitation are also presented in Figures 13(a) and 13(b). Doubling the excitation intensity has amplified the peak base shear force by 1.85 and the peak roof displacement by 2.89 as indicated in Figure 11. The corresponding response reduction factor, which can be

defined as the ratio of maximum elastic and inelastic base shear forces ($2/1.85$), is very close to 1 under a very severe excitation. Therefore, it is not worth consideration in seismic design.

The variation of the first storey damage index with time is calculated in the EW direction and presented in Figure 14. Damage accumulates quickly during the intense phase of excitation, then remains constant as

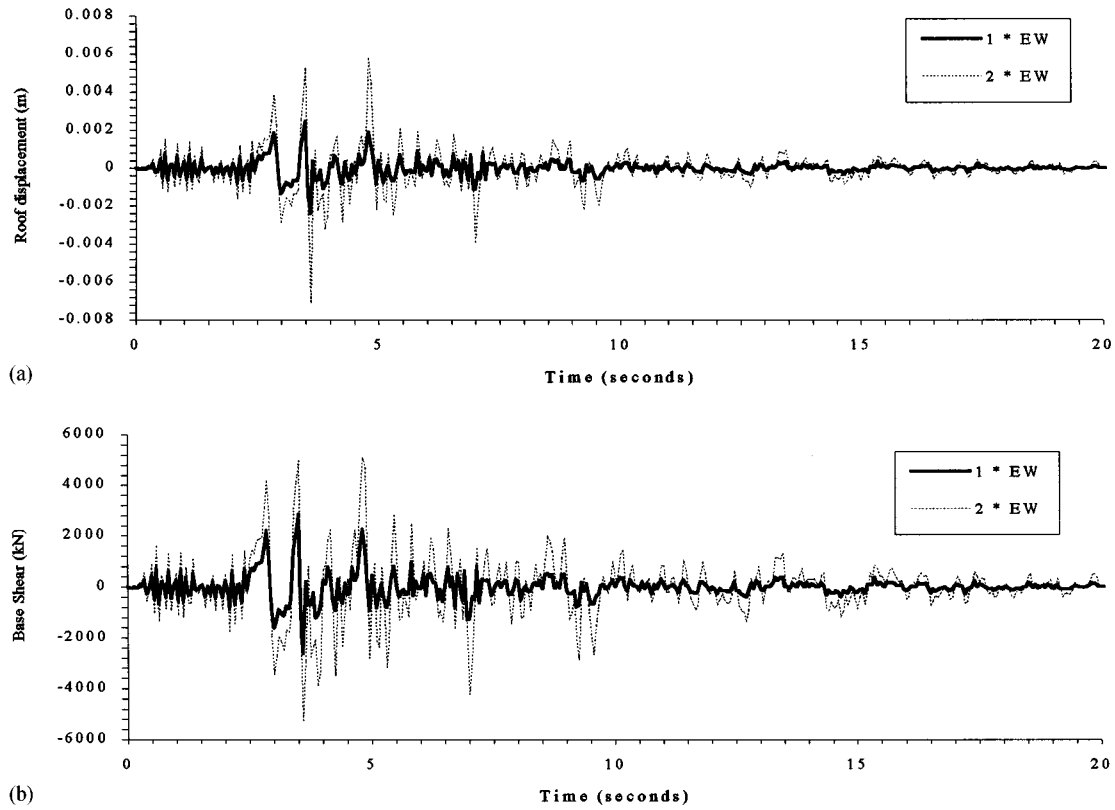


Figure 13. (a) Roof displacement time histories under both Erzincan EW component and Erzincan EW scaled by two. (b) Base shear force time histories under both Erzincan EW component and Erzincan EW scaled by two

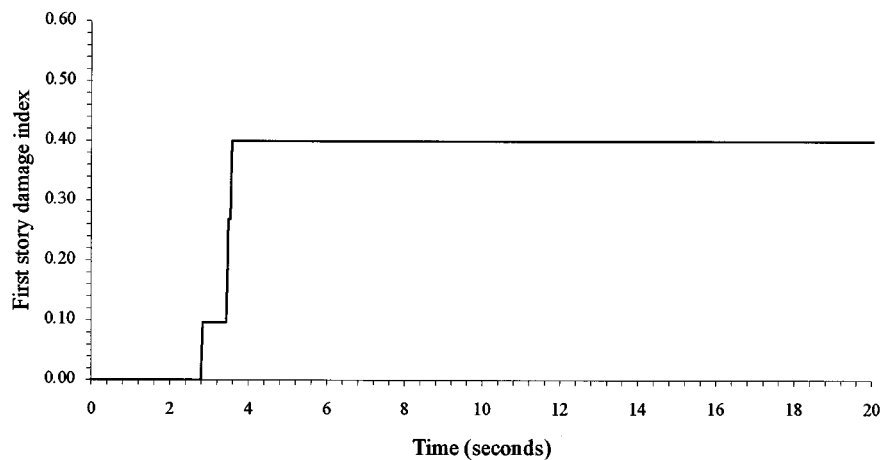


Figure 14. Progress of the first-storey damage index with time under Erzincan EW component scaled by two

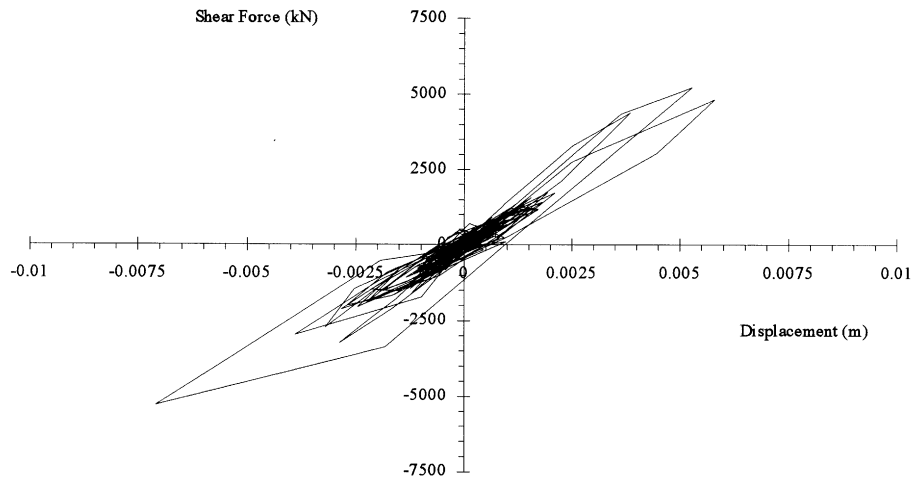


Figure 15. First-storey shear force-displacement relationship under Erzincan EW component scaled by two

expected. First storey of the building experiences moderate damage on the average under a ground excitation having a peak acceleration of 1.0 g. Heavy damage occurs in the first storey elements 8 and 9 (0.60); 10 and 11 (0.56); 4 (0.55) and 2 (0.52). First storey shear force-lateral displacement relationship in the EW direction is shown in Figure 15. Degradation in stiffness and increase in energy dissipation with increasing lateral displacement amplitudes can be observed. The damping ratio in the first storey wall elements associated with the maximum damage state varies between 0.15 (element 24) and 0.32 (elements 8, 9, 10, 11), with a storey average close to 0.25.

DISCUSSION OF RESULTS

The analytical results obtained by three different methods in the previous section, namely the modal spectrum analysis, incremental collapse analysis and time-history analysis, are compared in Figure 11. It can be observed that the capacity curves obtained by incremental collapse analysis trace the peak responses obtained by the other two methods accurately. Since this method requires substantially less computational effort than time-history analysis, capacity curves can be effectively used to determine the global level of safety possessed by a building under a seismic effect. The method is certainly more reliable for buildings where the lateral force distribution remains close to the assumed distribution shape during the actual inelastic dynamic response.

The difference between the modal spectrum analysis and time-history analysis in the linear elastic range is due to the effect of modal combination method, which is more pronounced in the EW direction where torsional coupling is significant.

Erzincan ground acceleration components (Figure 3) do not cause inelastic deformation and consequent damage in the building. This is consistent with the performance of the building during the 1992 earthquake. The EW component creates larger strains in the wall elements oriented in this direction and these strain values approach to the elastic strain limit (0.0005) in some elements. These elements are 8, 9, 10 and 11 with the corresponding strains of 0.000468, 0.000466, 0.000443 and 0.000444.

Increasing the intensity of EW ground shaking indicates first damage occurrence in elements 8 and 9 rather than the elements 10 and 11 where inclined plaster cracking was observed after the earthquake. This, contradiction can be explained in accordance with the mode of failure. The in-plane aspect ratios (height/length) of wall elements 8 and 9 are 3.6 and 4.2 whereas those of 10 and 11 are 1.4 and 1.2, respectively. Therefore, the dominant failure mode is flexure in elements 8, 9 and shear in elements 10, 11. The slender walls 8 and 9 can undergo lateral deformations larger than the squat elements 10 and 11 before

failure. Since the damage index employed in this study is based on shear deformations only, damage indices assigned to slender wall elements may be misleading. It should be remembered on the other hand that the contribution of slender elements to total lateral load resistance of the storey is insignificant.

The method of analysis presented in this study aims at assessing the basic seismic resistance mechanisms developed by unreinforced masonry buildings. It is revealed that masonry buildings have the advantages of remarkably high lateral resistance capacity and stiffness when they are constructed even with minimum material quality required by the seismic design codes. A uniform distribution of shear stresses can easily be achieved if a regular plan geometry is adopted and discontinuities in the walls leading to stress concentrations are avoided. Moreover, internal friction mechanisms in masonry walls lead to considerable energy dissipation capacity which further increases with increasing deformations. On the other hand, the observed disadvantage are the sudden progress of damage after attaining the ultimate strength state, accordingly the absence of a ductile, stable damaged state.

Unreinforced masonry buildings which survived earthquakes in the past withstood seismic forces mainly by their outstanding lateral resistance capacities. The ultimate capacity of the investigated building is almost equal to its weight, provided by its walls having areas less than 7 per cent of the plan area in each direction. This ratio exceeds 0.20 in many historical masonry buildings which have stood in earthquake countries for centuries.

A rational seismic design procedure for unreinforced masonry buildings can therefore be based on their elastic resistance limit, under the expected seismic forces which need not be reduced due to any permitted inelastic behaviour. The unused resistance capacity in this range should be kept as a safety reserve against variations in the material characteristics, workmanship and ground motion intensities.

A simple procedure is proposed here for checking the seismic safety of unreinforced masonry buildings. Since masonry buildings have usually short vibration periods, they receive elastic spectral forces specified in the acceleration amplification region of an elastic design spectrum. If maximum ground acceleration is specified as 0.40 g in a zone with the highest seismic activity,⁹ then spectral design acceleration for a short-period structure with 5 percent damping is 1.0 g. This value decreases to 0.75 g for 10 percent damping. Hence the base shear coefficient (V/W) can be taken as 0.75 for masonry buildings in the most severe seismic zone. Accordingly,

$$\frac{V_c}{W} > 0.75 \quad (8)$$

is required for a satisfactory seismic performance where V_c is the base shear force capacity.

The weight of a building can simply be approximated as

$$W = 10nA \quad (9)$$

where 10 has the unit of kN m^{-2} , n is the number of stories, and A is the plan area in m^2 . 10 kN m^{-2} is a reasonable estimate for the average weight of a storey per unit plan area. The base shear force capacity V_c is calculated at the elastic limit, which can be assumed as $\frac{2}{3}$ of the ultimate capacity at diagonal cracking, V_{cr} . Hence,

$$V_c = \frac{2}{3} V_{cr} \quad (10)$$

where

$$V_{cr} = \bar{\tau}_{av} A_{wi} \quad (11)$$

and A_{wi} is the wall area in a given direction. Cracking shear stress $\bar{\tau}_{av}$ is calculated by using a simplified version of equation (2)

$$\frac{\bar{\tau}_{av}}{f'_m} = \frac{\alpha}{1.6} \left(1 + 4 \frac{\sigma_y}{f'_m} \right) \quad (12)$$

where $\alpha = f'_t/f'_m$. Simplification of equation (2) is obtained by assuming $\alpha \ll 1$, $\sigma_y/f'_m \ll 1$ and approximating the square root term by binomial series expansion.¹⁷ Combining equation (8)–(12) and noting that $\sigma_y = W/A_w$ where A_w is the total wall area in both directions, which is $2A_{wi}$ for a regular building plan, the minimum necessary wall area ratio in each direction can be calculated as

$$\frac{A_{wi}}{A} \geq \frac{0.02}{\alpha} (0.9 - \alpha) \frac{n}{f'_m} \quad (13)$$

This equation may further be simplified with conservatism by ignoring the positive effect of vertical stress σ_y on diagonal cracking strength $\bar{\tau}$

$$\frac{A_{wi}}{A} \geq \frac{0.018}{\alpha} \cdot \frac{n}{f'_m} \quad (14)$$

The value of α varies in practice between 0.05 and 0.20, depending on the difference between compressive strengths of brick and mortar, and bond strength between the two constituents. Typically, for high strength factory bricks with compressive strength exceeding 30 MPa, α is less than 0.10. For low strength bricks having compressive strengths less than 10 MPa, α becomes larger than 0.15. If α can be estimated roughly, the only quantity required in equations (13) and (14) is the compressive strength of masonry which can be measured by testing masonry prism specimens.

When equation (14) is applied to the investigated building with $n = 3$, $f'_m = 3.95$ MPa and $\alpha = 0.182$ by using the properties presented in Tables I and II, it is found that the minimum A_w/A ratio should be 0.075 in both directions. Although the corresponding wall ratios are 0.065 and 0.061 in this building, it did not sustain any damage during the Erzincan earthquake. Such a result is not contradictory however, because the 10 per cent damped spectral accelerations produced by the Erzincan earthquake at the modal periods of the building are less than 0.75 g as shown in Figures 3(c) and 3(d). Moreover, the positive effect of vertical stress on shear strength is ignored in equation (14). If equation (13), which accounts for vertical stress was used instead, the minimum wall ratio would have been calculated as 0.06. This ratio is less than the supplied wall ratios indicated above.

CONCLUSIONS

Seismic performance of a multistorey unreinforced masonry building which survived a major earthquake without observable damage is evaluated comprehensively. Mechanical properties of the masonry walls have been determined through testing prism and panel specimens in the laboratory. Involved analytical methods are employed to predict the dynamic response of the building accurately. Following conclusions are derived from the presented study.

1. Unreinforced masonry buildings which satisfy basic seismic code requirements relevant to material strengths and geometric layout possess remarkable lateral load resistance both in the service (elastic) and ultimate limit states.
2. A balanced plan distribution of wall element leads to a uniform shear stress distribution in the elements where local concentration of stresses are avoided. Moreover, if diaphragm action is provided to ensure lateral displacement compatibility, a damaged wall element can redistribute its stresses to less damaged elements without impairing overall lateral resistance of the building.
3. Masonry buildings can provide a significant increase in their lateral resistance capacity between the elastic and ultimate resistance limits. The increase in the lateral resistance beyond elastic limit is accompanied by degradation in lateral stiffness and quick damage accumulation.
4. Masonry wall elements have considerable energy dissipation capacity through internal friction. The associated damping ratio further increases significantly when the elastic strain limit is exceeded.
5. A simple elastic design procedure can be adopted for the seismic design of unreinforced masonry buildings. Realistic damping ratios and material strengths should be employed in order to determine the seismic design forces and building resistance accurately. The increases in lateral strength and energy

dissipation capacities between the elastic and ultimate resistance limits should be considered as safety reserves against unexpected variations in seismic forces and material properties.

6. Out-of-plane bending behaviour of unreinforced masonry wall elements are not considered in this study. In this mode, no failures had been observed in the earthquake region for load-bearing unreinforced masonry walls under modest compression. However, this type of failure was common for infilled masonry separation walls not adequately tied in concrete frames.
7. The preceding conclusions are based on the non-linear analysis of a masonry building, facilitated by the material properties furnished by simple laboratory tests on similar materials. Since *in situ* mechanical properties of the investigated building are not available, the conclusions derived are limited to the validity of the assumptions employed in non-linear analysis.

REFERENCES

1. U.N. Development Program/U.N. Industrial Development Organization, 'Building construction under seismic conditions in the Balkan region. Design and construction of stone and brick masonry buildings', *UNDP/UNIDO Project RER/79/015*, Vienna, Austria, 1984.
2. M. Bruneau, 'State-of-the-art report on seismic performance of unreinforced masonry buildings', *J. struct. eng. ASCE* **120**, 230–251 (1994).
3. California Seismic Safety Commission, 'Damage to unreinforced masonry buildings in the Loma Prieta earthquake of October 17, 1989', Sacramento, California, 1991.
4. F. V. Karantoni and N. Fardis, 'Computed versus observed seismic response and damage of masonry buildings', *J. struct. eng. ASCE* **118**, 1804–1821 (1992).
5. F. Zaupa, C. Modena and S. Odorizzi, 'Evaluation of the safety level of existing buildings with particular reference to seismic actions', *Proc. 7th European conf. earthq. eng.*, European Assoc. of Earthq. Eng., Vol. 5, 1987, 157–171.
6. H. Sucuoğlu and M. Tokyay (eds), 'Engineering report of the 13 March 1992 Erzincan earthquake', Chamber of Civil Eng., Ankara, June 1992 (in Turkish).
7. Ministry of Settlement and Reconstruction, 'Regulations for buildings in disaster areas', Ankara, 1968 (in Turkish).
8. Turkish Standards Institute, 'Design and construction rules for masonry walls', Ankara, TS 2510, April 1977 (in Turkish).
9. Uniform Building Code, *International Conference of Building Officials*, Whittier, California, 1991.
10. F. Y. Yokkel and S. G. Fattal, 'Failure hypothesis for masonry shear walls', *J. struct. div. ASCE* **102**, 515–532 (1976).
11. K. Tanrikulu, Y. Mengi and H. D. McNiven, 'The non-linear response of unreinforced masonry buildings to earthquake excitations', *Earthquake eng. struct. dyn.* **21**, 965–985 (1992).
12. Y. Mengi, H. D. McNiven and A. K. Tanrikulu, 'Models for nonlinear earthquake analysis of brick masonry buildings', *Report No. UCB/EERC-92/03*, Earthquake Eng. Res. Center, University of California, Berkeley, CA, 1992.
13. M. Tomazevic, 'Dynamic modelling of masonry buildings: storey mechanism model as a simple alternative', *Earthquake eng. struct. dyn.* **15**, 731–749 (1987).
14. D. Benedetti and G. M. Benzon, 'A numerical model for seismic analysis of masonry buildings: experimental correlations', *Earthquake eng. struct. dyn.* **12**, 817–831 (1984).
15. Y. Mengi and H. D. McNiven, 'A mathematical model for the in-plane non-linear earthquake behavior of unreinforced masonry walls, Part 1: experiments and proposed model', *Earthquake eng. struct. dyn.* **18**, 233–247 (1989).
16. H. D. McNiven and Y. Mengi, 'A Mathematical model for the in-plane non-linear earthquake behavior of unreinforced masonry walls, Part 2: completion of the model', *Earthquake eng. struct. dyn.* **18**, 249–261 (1989).
17. H. Sucuoğlu and H. D. McNiven, 'Seismic shear capacity of reinforced masonry piers', *J. struct. eng. ASCE* **117**, 2166–2186 (1991).
18. V. Turnsek and F. Cavocic, 'Some experimental results on the strength of brick masonry walls', *Proc. 2nd int. brick masonry conf.*, Stoke-on-Trent, 1970.
19. A. A. Hamid and R. G. Drysdale, 'Concrete masonry under combined shear and compression along the mortar joints', *ACI j.*, September, October, 314–319 (1980).
20. B. Sveinsson, H. D. McNiven and H. Sucuoğlu, 'Cyclic loading tests of masonry single piers-Vol. 4: additional tests with height to width ratio of 1', *Report No. UCB/EERC-85/15*, Earthquake Eng. Res. Center, University of California, Berkeley, CA, 1985.